



Single-pulse resonant magnetic scattering using a soft x-ray free-electron laser

C. Gutt,¹ S. Streit-Nierobisch,¹ L.-M. Stadler,¹ B. Pfau,^{2,3} C. M. Günther,^{2,3} R. Könnecke,^{2,3} R. Frömter,⁴ A. Kobs,⁴ D. Stickler,⁴ H. P. Oepen,⁴ R. R. Fäustlin,¹ R. Treusch,¹ J. Feldhaus,¹ E. Weckert,¹ I. A. Vartanyants,¹ M. Grunze,^{5,6} A. Rosenhahn,^{5,6} T. Wilhein,⁷ S. Eisebitt,^{2,3} and G. Grübel¹

¹Deutsches Elektronen-Synchrotron (DESY), Notkestr. 85, D-22607 Hamburg, Germany

²Helmholtz-Zentrum Berlin für Materialien und Energie GmbH, Hahn-Meitner Platz 1, D-14109 Berlin, Germany

³Institut für Optik und Atomare Physik, TU Berlin, Hardenbergstr. 36, D-10623 Berlin, Germany

⁴Institut für Angewandte Physik, Jungiusstr. 11, D-20355 Hamburg, Germany

⁵Angewandte Physikalische Chemie, Universität Heidelberg, Im Neuenheimer Feld 253, D-69120 Heidelberg, Germany

⁶Institute of Toxicology and Genetics (ITG), Forschungszentrum Karlsruhe, P.O. Box 3640, D-76021 Karlsruhe, Germany

⁷Institute for X-ray-Optics, RheinAhr-Campus Remagen, FH Koblenz, Südallee 2, D-53424 Remagen, Germany

(Received 4 December 2009; revised manuscript received 7 January 2010; published 1 March 2010)

We report on single-pulse resonant magnetic scattering experiments using soft x-ray pulses generated by the free-electron laser FLASH at DESY. We could record a magnetic diffraction pattern from a Co/Pt multilayer sample at the Co $M_{2,3}$ edge with a single 30-fs-long FEL pulse. The analysis of the magnetic small-angle scattering signal for subsequent pulses indicates a threshold energy density below which there is no indication that the magnetic properties of the sample might be altered.

DOI: [10.1103/PhysRevB.81.100401](https://doi.org/10.1103/PhysRevB.81.100401)

PACS number(s): 75.70.-i, 78.70.Ck, 41.60.Cr

Free-electron laser (FEL) sources based on self-amplified spontaneous emission (SASE) (Ref. 1) can provide intense and ultrashort (femtosecond) pulses from the vacuum ultraviolet (VUV) to the x-ray range. These sources have the potential to record a magnetic diffraction pattern from a sample within a few femtosecond exposure and thus to probe elementary magnetization dynamics such as spin-flip processes and their coupling to the electronic system on their intrinsic time scales in the femtosecond (fs) regime.²⁻⁵ At the same time nanometer spatial resolution and element-specific information is provided allowing to access the complex composition of technologically relevant magnetic media and devices.

However, the unprecedented peak power of FEL sources also implies that a considerable amount of energy is deposited in the sample. The radiation damage threshold defines the borderline between nondestructive and therefore repeatable pump-probe type of magnetic scattering experiments and high fluence destructive single-pulse experiments. Single-pulse (nonmagnetic) scattering of simple amplitude objects has been demonstrated recently.^{6,7} It has been shown that a diffraction pattern of an unperturbed sample can be recorded fast enough before the sample is destroyed in a Coulomb explosion. Photoionization is the dominant absorption mechanism at the wavelength considered here. Photoemission is followed by Auger or fluorescence emission and shake up or down excitations.⁸ These electrons are released at different times but within about 10 fs following photoabsorption.⁸ Thermalization of the ejected electrons through collisional electron cascades is completed within 10–100 fs. Heat transport and diffusion take place over some picoseconds to milliseconds.

Beam damage renders single-pulse scattering from magnetic samples especially challenging as one would ideally take femtosecond snapshots without modifying samples. The resonant magnetic scattering mechanism has its origin in the virtual excitation of a core-level electron to an unoccupied

spin-polarized state above the Fermi level which decays with the emission of a photon. It is therefore element-specific and sensitive to spin orientations. It has been shown that the spin system can be quenched on time scales of 50–100 fs using high-fluence optical laser pulses^{2,3} and a similar process may happen during the femtosecond exposure to a soft x-ray FEL beam making ultrafast scattering impossible. Moreover, high fluences may also alter the magnetic properties of multilayer films as has been reported in Ref. 9.

In order to address these issues, we performed single-pulse resonant magnetic diffraction experiments at the soft x-ray free-electron laser FLASH in Hamburg.^{10,11} We demonstrated recently the first resonant magnetic scattering at FLASH by using the fifth harmonic of 8 nm to obtain magnetic scattering contrast at the Co L_3 edge.¹² Now, the fundamental wavelength was set to 20.8 nm (59 eV) which is in resonance with the Co $M_{2,3}$ -edge yielding magnetic scattering contrast. FLASH was operated in single-bunch mode with a repetition rate of 5 Hz. The pulse duration was 30 fs with an average pulse intensity of 2 μJ which corresponds to 2×10^{11} photons/pulse on the sample in a beam size of 250 μm . This results in a photon fluence of 4 mJ/cm^2 and peak powers of about 1.3×10^{11} W/cm^2 . The experiment has been performed at beamline BL1 at FLASH which utilizes the direct FEL beam without monochromator. The natural bandwidth of the SASE radiation $\Delta E/E \approx 0.5\% - 1\%$ is sufficiently small to allow for resonant scattering at the Co M edge. A toroidal mirror produces a beam size of about 150 μm in the focal plane. Our samples have been positioned slightly out of focus resulting in the beam size of around 250 μm on the samples.

The samples have been mounted in a vacuum chamber equipped with a photon absorber, photodiode, and sample translation stages. The scattered photons are detected by a soft x-ray in-vacuum charge-coupled device (CCD) camera (Princeton PI-MTE) mounted at a distance of 4 cm from the samples (schematic setup shown in Fig. 1). The camera has

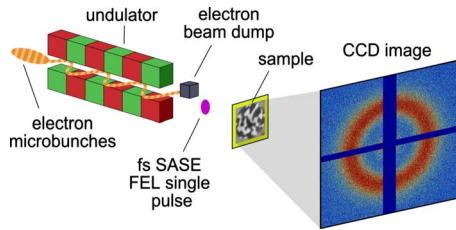


FIG. 1. (Color online) Schematics of the single-pulse magnetic scattering setup.

2048 × 2048 pixels of 13.5 microns size and is triggered by the FEL fast shutter signal allowing for single-pulse recording. A wire beamstop of 1 mm diameter blocks the transmitted beam.

Co/Pt multilayer samples were grown via magnetron sputtering on a 50-nm-thick Si₃N₄ membrane. A 5-nm-thick ECR sputtered Pt layer serves as seed layer,¹³ followed by 16 repeats of [Co (0.8 nm)/Pt (1.4 nm)] and a final Pt cap layer of 2 nm thickness, all prepared by dc magnetron sputtering.¹⁴ The sample is mounted in such a way that the FEL beam is impinging on the membrane first before being scattered from the multilayer. In multilayer samples of this composition magnetic maze domains form with alternating up and down magnetization perpendicular to the sample surface. The spatial correlation of the domains, being twice the domain size, is on the order of 200–300 nm leading to a pronounced magnetic small-angle scattering (SAXS) signal.

The resonant electrical dipole scattering amplitude f_n is given for each lattice site n by¹⁵

$$f_n = \mathbf{e}' \cdot \mathbf{e} F_n^c - i(\mathbf{e}' \times \mathbf{e}) \cdot \mathbf{M}_n F_n^{m1} + (\mathbf{e}' \cdot \mathbf{M}_n)(\mathbf{e} \cdot \mathbf{M}_n) F_n^{m2}, \quad (1)$$

where \mathbf{e} and \mathbf{e}' denote the polarization vectors of the incident and scattered radiations, respectively, F_n^c is the anomalous charge scattering factor, \mathbf{M} is the unit vector of the magnetization, and the complex transition matrix elements $F_n^{m1,2}$ describe the resonant atomic excitation and decay process. For a comparison of the magnetic scattering cross sections at L and M edges of Co see Refs. 16 and 17. The first term in Eq. (1) is irrelevant for our sample since no charge heterogeneities exist on the addressed length scales.^{18–20} The second term shows a nonvanishing amplitude for scattering from linear polarization \mathbf{e} to perpendicular polarization \mathbf{e}' with varying contrast according to whether $\mathbf{e} \times \mathbf{e}'$ is parallel or antiparallel to a magnetic domain orientation. As the magnetization is perpendicular to the polarization of the x rays, the third term does not contribute to the scattered intensity $I(Q)$. $I(Q)$ is then given as a sum over the lattice sites n located at r_n , $I(Q) = |\sum_n f_n \exp(iQr_n)|^2$. Within a magnetic domain all lattice sites provide the same scattering amplitude thus the scattered intensity reflects the structure factor $S(Q)$ of the magnetic domains, i.e., $I(Q) \propto S(Q)$.

Figure 2 shows a resonant magnetic SAXS pattern recorded with a 30-fs-long single FEL pulse of pulse energy 4 μ J. A subsequent illumination showed that the sample was not destroyed from the single-pulse exposure. The scattering ring reflecting the spatial correlation via $\xi = 2\pi/Q_{max} = 200$ nm of the magnetic domains is clearly visible (see

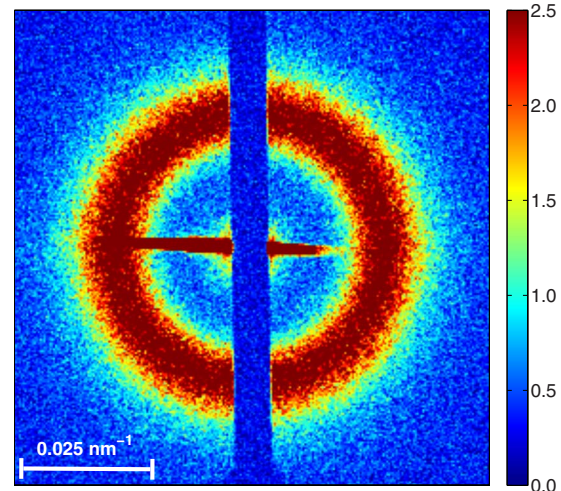


FIG. 2. (Color online) Resonant magnetic small-angle scattering pattern of a Co/Pt multilayer recorded with a single 30 fs FEL pulse of 1.3×10^{11} W cm⁻². The photon wavelength was in resonance with the Co $M_{2,3}$ edge (20.8 nm) providing magnetic scattering contrast. The color scales indicates the number of scattered photons per pixel (4×4 binned image).

also Ref. 12). The existence of magnetic scattering proves that the spin system temperature is below the Curie temperature of the multilayer sample during the exposure time. It is worth mentioning that even FEL pulse energies 10–20 times larger than the one applied here allowed us to record a single-pulse magnetic diffraction pattern. Those high pulse energies destroyed the sample although the spin system is still not quenched *during* the exposure time of 30 fs.

Having recorded a single-pulse magnetic diffraction pattern we investigated also the influence of the high fluence on the magnetic properties of the magnetic multilayer. For this purpose the same sample was irradiated with 30 single pulses. Figure 3 shows a series of magnetic diffraction patterns taken from the same sample spot. Each pattern was acquired with a single 30-fs-long FEL pulse. The time delay between the images is around 3–10 s. In average each pixel

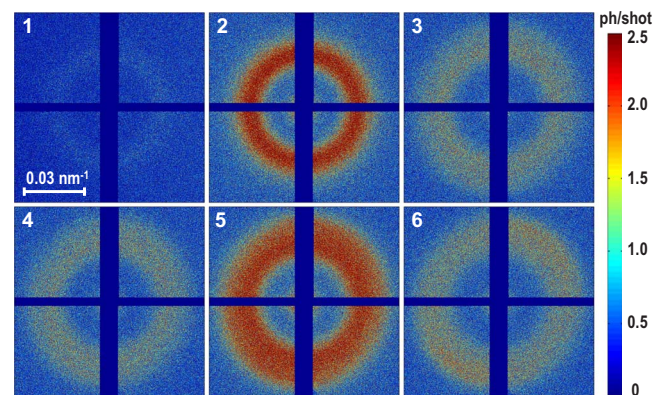


FIG. 3. (Color online) Magnetic small-angle scattering patterns from six subsequent 30 fs illuminations of the same Co/Pt multilayer sample, from one single FEL pulse each. The time delay between the images is 10 s. The color scale indicates the number of scattered photons per pixel.

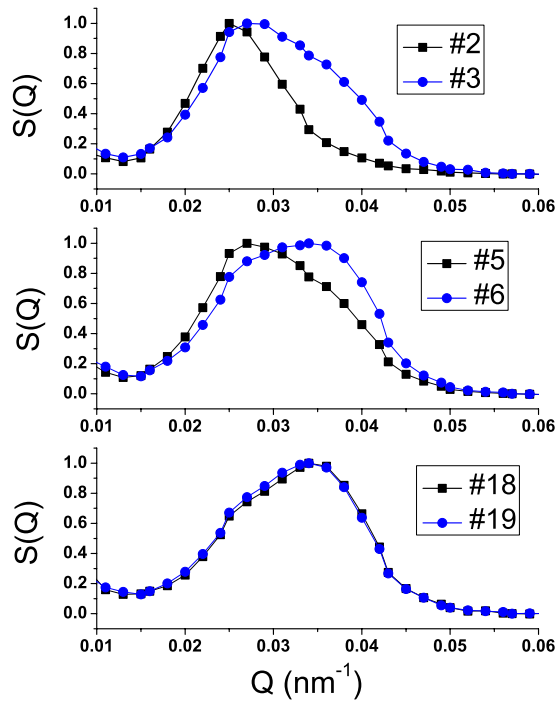


FIG. 4. (Color online) The magnetic structure factor $S(Q)$ of the domain structure for different pulses as deduced from the CCD images.

of the SAXS ring contains around 1–2 scattered photons per single pulse. Due to the statistical nature of the SASE process¹ the FEL pulse energy was higher for pulse 2 and 5 than for the rest of the images. The SAXS ring from the magnetic domains is visible in the first two images at $Q_{\max} = 0.026 \text{ nm}^{-1}$ reflecting a mean domain size of around 120 nm in the sample. After the higher intensity of pulse 2 the third image shows a larger and broader ring, and after the second high-intensity shot (5) the maximum of the ring in image 6 is again shifted to larger Q values.

This is quantified by the azimuthally integrated structure factor $S(Q)$ of the magnetic domains, which is shown for selected pulse numbers in Fig. 4. For reasons of comparison the structure factors have been normalized. A change in both the peak positions Q_{\max} and the line shapes as a function of pulse number is clearly visible. Especially strong changes in $S(Q)$ occur from pulse 2 to 3 and from pulse 5 to 6. The structure factor shifts to larger Q values (smaller domain sizes) and becomes broader. However, there are also pulses which induce no change in the magnetic structure factor (e.g., pulse 18 to 19).

The changes in $S(Q)$ can be attributed to high-intensity FEL pulses hitting the sample and altering the magnetic properties of the multilayer sample. Figure 5 displays the scattering intensity (top) and the average domain size (bottom) as a function of pulse number. The stochastic nature of the SASE process leads to fluctuations in the incoming pulse intensity. Pulses 2 and 5 provide high-intensity scattering patterns with 2.6 and 2.3 photons per pixel, respectively. We estimate from the average SASE pulse energy that 1 scattered photon per pixel, averaged over the SAXS ring, corresponds to FEL pulse energies of $2 \mu\text{J}$ ($4 \text{ mJ}/\text{cm}^2$). After

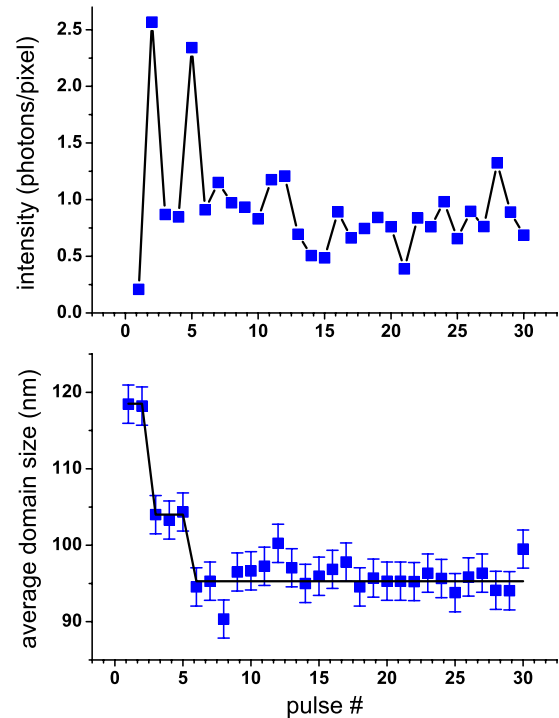


FIG. 5. (Color online) Top: maximum scattered intensity per pixel as a function of pulse number. Bottom: average magnetic domain size as a function of pulse number.

those high photon flux pulses the following pulses 3 and 6 reveal drastic changes in $S(Q)$. The domain size decreases between 2 and 3 from 120 to 105 nm and then again between pulses 5 and 6 from 105 to 95 nm. After these two high-intensity pulses the magnetic domain size stays constant within the error bar. Other samples confirmed the picture of high-intensity FEL pulses inducing changes in the domain size distribution.

The observed changes in $S(Q)$ are caused by permanent changes in the structure of the magnetic multilayer. SEM pictures of both unirradiated and irradiated areas of the sample revealed an increase in the grain size upon irradiation with the FLASH pulse. From irradiation experiments with ions and ns long intense laser pulses it is known that the deposited energy can change grain sizes or the interfacial structure of layers, leading to a reduction in the perpendicular magnetic anisotropy.^{9,21,22} A decrease in perpendicular anisotropy reduces the energy per domain wall length and thus shifts the equilibrium domain size toward smaller values.²³ The process of atomic diffusion and interfacial structure changes happens on time scales much longer than the exposure time of the FEL pulse. Following Ref. 24 we estimate that during the 30-fs-long exposure the Co and Pt atoms move less than 0.01 nm so that interlayer diffusion during the exposure can be neglected. Therefore changes to the magnetic structure become only apparent at the next exposure to the FEL beam.

We estimate the peak temperatures of the multilayer by calculating the target depth-dependent total-energy deposition. For this purpose the multilayer has been divided into equidistant cells with specific material opacities.²⁵ The tem-

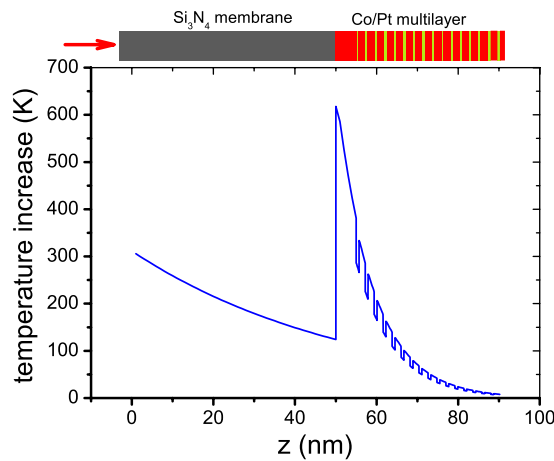


FIG. 6. (Color online) Calculation of the temperature change in the magnetic multilayer sample 1 ps after irradiation by the FEL pulse as a function of lateral position z in the sample (pulse energy 4 mJ/cm^2). For details see text. The FEL pulse is incident on the 50-nm-thick silicon nitride membrane from the left. The Pt seed layer starts at $z=50 \text{ nm}$.

perature change (Fig. 6) is then obtained via the room-temperature heat capacity, which is assumed to remain constant throughout the interaction period between the FEL pulse and the magnetic multilayer. This yields a relatively good approximation for equilibrated systems (i.e., time scales $\geq 1 \text{ ps}$) and low deposited energy densities so that in our case the target crystal lattice does not undergo significant transitions. Here, the calculated maximum energy deposition

is 2 kJ/cm^3 , which is sufficiently lower than the specific melting energy [4.4 kJ/cm^3 (Ref. 26)] and the first ionization energy [68 kJ/cm^3 (Ref. 26)]. Heat transport, which also occurs on nm spatial scale and would wash out the curve in Fig. 6, is not taken into account. Thus, the calculation gives an estimate on the target condition $\approx 1 \text{ ps}$ after irradiation. From the calculation we estimate that the magnetic multilayer reaches peak temperatures of around $600 \text{ }^\circ\text{C}$ for pulse energies of 4 mJ/cm^2 and $1400 \text{ }^\circ\text{C}$ for 9.2 mJ/cm^2 . In the latter case the deposited energy leads to permanent changes in the structure of the multilayer film. The structural changes *alter* atomic positions at the interface. Via the interface contributions to the magnetic anisotropy, the intrinsic domain width of the multilayer system is thus altered. As an additional effect, pinned domain walls forming a magneto-statically metastable state may be released due to thermal activation after the FLASH pulse.

In conclusion, we demonstrated nondestructive resonant magnetic scattering using single pulses from the free-electron laser FLASH. Pulse energies of 4 mJ/cm^2 are sufficient to record a magnetic diffraction pattern within 30 fs without destroying the sample. We observed that higher pulse intensities can lead to permanent changes of the magnetic properties of the magnetic multilayer but without macroscopically observable destruction. Below that threshold it is possible to record magnetic diffraction patterns without changing the magnetic domain size distribution.

Financial support by Free and Hanseatic City of Hamburg in the context of the Landesexzellenzinitiative Hamburg, and by DFG within SFB 668 is gratefully acknowledged.

- ¹E. L. Saldin, E. A. Schneidmiller, and M. V. Yurkov, *The Physics of Free Electron Lasers* (Springer, Berlin, 1999) and references therein.
- ²E. Beaurepaire, J.-C. Merle, A. Daunois, and J.-Y. Bigot, *Phys. Rev. Lett.* **76**, 4250 (1996).
- ³L. Guidoni, E. Beaurepaire, and J. Y. Bigot, *Phys. Rev. Lett.* **89**, 017401 (2002).
- ⁴A. V. Kimel, A. Kirilyuk, and T. Rasing, *Laser Photonics Rev.* **1**, 275 (2007).
- ⁵C. Stamm, T. Kachel, N. Pontius, R. Mitzner, T. Quast, K. Holl-dack, S. Khan, C. Lupulescu, E. F. Aziz, M. Wietstruk, H. A. Dürr, and W. Eberhardt, *Nature Mater.* **6**, 740 (2007).
- ⁶H. N. Chapman *et al.*, *Nat. Phys.* **2**, 839 (2006).
- ⁷A. Barty, S. Boutet, M. J. Bogan, S. P. Hau-Riege, S. Marchesini, K. Sokolowski-Tinten, N. Stojanovic, R. Tobey, H. Ehrke, A. Cavalleri, S. Düsterer, M. Frank, S. Bajt, B. W. Woods, M. M. Seibert, J. Hajdu, R. Treusch, and H. N. Chapman, *Nat. Photonics* **2**, 415 (2008).
- ⁸R. Neutze, R. Wouts, D. van der Spoel, E. Weckert, and J. Hajdu, *Nature (London)* **406**, 752 (2000).
- ⁹C. Schuppler, A. Habenicht, I. L. Guhr, M. Maret, P. Leiderer, J. Boneberg, and M. Albrecht, *Appl. Phys. Lett.* **88**, 012506 (2006).
- ¹⁰K. Tiedtke *et al.*, *New J. Phys.* **11**, 023029 (2009).
- ¹¹W. Ackermann *et al.*, *Nat. Photonics* **1**, 336 (2007).
- ¹²C. Gutt *et al.*, *Phys. Rev. B* **79**, 212406 (2009).
- ¹³M. Wellhöfer, M. Weißenborn, R. Anton, S. Pütter, and H. P. Oepen, *J. Magn. Magn. Mater.* **292**, 345 (2005).
- ¹⁴H. Stillrich, C. Menk, R. Frömter, H. P. Oepen, J. Magn. Magn. Mater. (to be published).
- ¹⁵J. P. Hannon, G. T. Trammell, M. Blume, and D. Gibbs, *Phys. Rev. Lett.* **61**, 1245 (1988).
- ¹⁶H. C. Mertins, F. Schäfers, X. Le Cann, A. Gaupp, and W. Gudat, *Phys. Rev. B* **61**, R874 (2000).
- ¹⁷S. Valencia, A. Gaupp, W. Gudat, H. C. Mertins, P. M. Oppeneer, D. Abramsohn, and C. M. Schneider, *New J. Phys.* **8**, 254 (2006).
- ¹⁸J. B. Kortright, S.-K. Kim, G. P. Denbeaux, G. Zeltzer, K. Takano, and E. E. Fullerton, *Phys. Rev. B* **64**, 092401 (2001).
- ¹⁹S. Eisebitt, J. Lüning, W. F. Schlotter, M. Lörger, O. Hellwig, W. Eberhardt, and J. Stöhr, *Nature (London)* **432**, 885 (2004).
- ²⁰O. Hellwig, A. Berger, J. B. Kortright, and E. E. Fullerton, *J. Magn. Magn. Mater.* **319**, 13 (2007).
- ²¹C. Chappert *et al.*, *Science* **280**, 1919 (1998).
- ²²M. J. Bonder, N. D. Telling, P. J. Grundy, C. A. Fauce, T. Shen, and V. M. Vishnyakov, *J. Appl. Phys.* **93**, 7226 (2003).
- ²³M. Speckmann, H. P. Oepen, and H. Ibach, *Phys. Rev. Lett.* **75**, 2035 (1995).
- ²⁴S. P. Hau-Riege *et al.*, *Phys. Rev. Lett.* **98**, 145502 (2007).
- ²⁵B. Henke, E. Gullikson, and J. Davis, *At. Data Nucl. Data Tables* **54**, 181 (1993).
- ²⁶D. R. Lide, *CRC Handbook of Chemistry and Physics*, 88th ed. (CRC Press LLC, Boca Raton, FL, 2007).